Improving the optical and dielectric properties of PVA matrix with nano-ZnSe: Synthesis and Characterization

[1]Jobin Job Mathen, [2]Ginson P. Joseph, [3]J. Madhavan
[1,3]Department of Physics, Loyola College, Chennai, India
[2]Department of Physics, St. Thomas College, Palai, India

Abstract **- ZnSe/Poly (vinyl alcohol) (PVA) composite membranes with 30 – 40 µm thicknesses were prepared by ultra-sonication technique at different weight percentages (0-4%) of ZnSe nanoparticles. The structural characteristic of synthesized ZnSe was examined by X-ray analysis. The surface morphology and the formation of composite membrane were displayed in SEM micrographs. Important dielectric parameters which include dielectric constant, dielectric loss and electric modulus were exemplified and three different relaxation mechanisms were identified during heat treatment. The dielectric constant was increased from (k = 7.02, 100Hz, 30^{0}C) to (k = 16.02, 100Hz, 120^{0}C) and the composite films exhibited a higher energy storage efficiency, that is an increase of 49.7% (at 1MHz) was noticed in the case of 4%ZnSe/PVA. The index of refraction and optical conductivity could be enhanced with the inclusion of ZnSe nanoparticles within percolation threshold. Thus, these high n and k–ZnSe/PVA nano composites are potential flexible high-performance dielectric materials for electronic devices.**

Index Terms **- ZnSe, electric modulus, index of refraction, dielectric material.**

I. INTRODUCTION

The advances in the fundamental materials science lead to the development of new functional materials or new combination of existing materials, which exhibit superior electrical and optical properties. Researchers are enforced to focus on composites which consist of polymer as host matrix and semiconductor particles as filler due to the practical interest towards the better electrical, optical and mechanical properties of individuals and its dielectric, ferroelectric and piezoelectric properties are widely used in various applications [1-4]. Recently, composite membranes are becoming prominent candidates in an intensive development of transducers, energy harvesting devices, underwater hydrophones, embedded capacitors, high-pressure sensors, biomedical imaging and non-destructive testing applications [5-7]. The most important materials used for wireless communication devices are microwave dielectric materials with appropriate permittivity, low dielectric loss and a suitable temperature coefficient of resonant frequency [8]. It is for this reason that composite dielectrics and its electrical and optical properties have been so intensively investigated. Moreover, there is easiness in the preparation of polymer/semiconductor composite with diverse properties and hence tailor the properties as per requirements.

Among different polymers, poly (vinyl alcohol) (PVA) attracted the attention of researchers due to its optical characteristics, physical properties, film forming and biocompatibility. Furthermore, its properties still appear to be unique in terms of the price/performance ratio. To further enhance the properties, the incorporation of inorganic material is advantageous for forming a composite which could be lightweight, flexible and exhibit good moldability [9]. The properties of semiconductor nanoparticles depend mainly on their shape and size due to their high surface to volume ratio [10-12]. Zinc Selenide (ZnSe) is a non-hygroscopic, chemically stable and wide band gap semiconductor that has an excellent dielectric and optical properties like excellent luminescence efficiency, low absorption coefficient and excellent transparency to infra-red [13-15]. The II-VI semiconductors have used in many applications such as light emitting diodes, acousto-optical effects and biological sensors [16-19]. Technologies are demanding materials with improved structural, electrical and chemical modifications of traditional PVA with the addition of good inorganic materials like ZnSe for the development of new nano devices. In the present study, we have made an attempt to prepare ZnSe/PVA composite films by ultra-sonication technique. The morphological, optical and dielectric properties of ZnSe/PVA nanocomposite films of 30-40 µm thickness are exemplified.

II. MATERIALS AND METHODS

Materials

Materials used for the preparation of ZnSe nanopowders are Merck GR grade of purity ≥ 98%. The materials used are Zinc acetate dihydrate ($Zn(O_2CCH_3)_2(H_2O)_2$), sodium selenite (Na_2SeO_3), hydrazine hydrate ($N_2H_4.H_2O$) and PVA resin (white) $[CH_2CHOH]_n$.

Synthesis of ZnSe nanoparticles

Zinc acetate of 4.388g was dissolved in 100 ml of direct Millipore water and 0.519g of sodium selenite (Na_2SeO_3) was dissolved in 30 ml of hydrazine hydrate ($N_2H_4.H_2O$). Both the prepared solutions were mixed under vigorous stirring with

external heat energy at 60℃. These solutions were poured into a Teflon lined sealed stainless steel autoclave and heated at 210℃ for 6 hours in a muffle furnace and then cooled to room temperature naturally. The precipitate was collected by centrifugation, washed twice using distilled water for removing impurities and dried to obtain ZnSe nano powders.

Synthesis of ZnSe/PVA nanocomposites

ZnSe/PVA nanocomposites were prepared at different weight percentages (0-4%) of as-synthesized ZnSe nanoparticles by ultra-sonication method. Poly (vinyl alcohol) (PVA) is a water soluble polymer and hence it was dissolved in hot water with gentle stirring for one hour. Next, to obtain a homogeneous dispersion of ZnSe nanoparticles in PVA-water mixture, magnetic stirring and ultra-sonication were used. The ZnSe-PVA solution was transferred into a Teflon coated glass mold to acquire a thin film of 30 – 40 µm thicknesses. The mold assembly was then kept in air-oven at 50 ℃ for 4 hours to obtain the nanocomposite thin films by volatilizing water.

Characterization

The X-ray diffraction (XRD) pattern was used to confirm the structure and to obtain the particle size of ZnSe particles. The patterns were recorded in the two theta (2θ) range of 2.0°-70° using a Bruker-D8-AXS diffractometer system equipped with a CuK_α radiation (λ=1.5406 A˚). The morphology of the obtained composites was analyzed using a JEOL JSM-6390 LV scanning electron microscopy (SEM). The UV- Vis- NIR spectroscopy is fruitful for characterizing the optical properties of the material. The UV- Vis- NIR absorbance spectrum of composite membranes was recorded using Varian Cary 5000 UV-Vis-NIR Spectrophotometer in the range of 200 to 900 nm. The dielectric measurements were carried out using HIOKI LCR impedance analyzer 3532-50 in the frequency range of 100 Hz to 1 MHz by varying the temperature up to 120°C.

III. RESULTS AND DISCUSSION

XRD Analysis

Structural characterization of ZnSe nanoparticles was carried out by X-ray diffraction analysis. Fig. 1 shows XRD pattern of obtained particles with molar concentration Zn:Se is 2:1. Figure shows the localized peaks at 2θ = 25.8°, 45.0° and 53.8° are related to ZnSe, according to JCPDS card no: 80-0021, corresponding to the crystallographic planes (1 1 1), (2 2 0) and (3 1 1). A very small peak is observed at 2θ = 65.9° which corresponds to the plane (4 0 0). The particle size is estimated from XRD pattern using the Debye-Scherrer equation [20] and an average size are between 9.5 nm to 13.8 nm. The calculated particle size is in good agreement with the diametrical size obtained from SEM image.

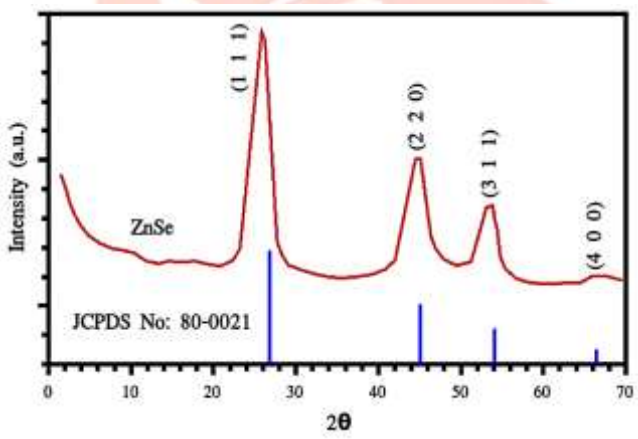

Fig. 1: XRD pattern of as-synthesized ZnSe nanoparticles.

Morphological analysis

SEM micrographs have a very large depth of field yielding a characteristic three dimensional appearance which is useful for understanding the surface morphology of the sample. The SEM micrographs of 4%ZnSe/PVA thin film are shown in fig. 2, at different magnification of 3,300X and 95,000X. One of the images shows the distribution of ZnSe nanoparticles on the host matrix and revealed some particles aggregate within the polymer membrane. Apparently, the results inferred that the addition of 4% (wt %) ZnSe tend to cause the aggregation but could reduce the inter-particle distance as the density of the host matrix is treated as constant. An enhanced tunneling conduction is expected with the increase in the dopant concentration. The magnified surface view shows that the size of the as-synthesized ZnSe particle is about 24 nm.

Dielectric properties

The dielectric measurements have been carried out by a capacitive arrangement technique using HIOKI LCR impedance analyzer 3532-50 in the frequency range of 100 Hz to 1 MHz and within the temperature 30ºC to 120ºC. The polarized molecules or atoms in dielectric medium can align in accordance with the applied electric field which implies electromagnetic energy to be transferred into materials. Fig. 3 shows the behavior of frequency dependent dielectric constant of PVA and ZnSe/PVA at room temperature. The plot inferred that the value of dielectric constant has a strong influence in radio frequency region. At lower frequencies, high values are noticed which indicate that the four polarizations are active whereas at higher frequencies, due to the high periodic field reversal resulting in an inertia of the dipolar moments causes the reduction in the values. An independent frequency trace is noticed beyond 1

kHz but a substantial modification is achieved by the incorporation of ZnSe nanoparticles in the matrix. A giant polarizability is noticed because the particles are relatively free to move in extended trajectories between the electrodes. The ZnSe exhibits a strong ionic polarization due to Zn^{2+} and Se^{2-} ions and has a high value of static permittivity so that the increment in the values of relative permittivity for the composites due to these mobile charge carriers is expected. For pure PVA and 4%ZnSe/PVA, it is 7.02 and 11.08 respectively at 100Hz. This study is extended to the temperature variation up to 120°C. Fig. 4 displays the variation in relative permittivity values in accordance with the temperature. At higher temperatures, the intermolecular forces between the polymer chains are broken and it will be free to orient with the periodic electric field thus higher relative permittivity.

Fig.5 illustrates the frequency dependent dielectric loss of PVA and its composites at room temperature. This curve possessed a similar trace as the plot of dielectric constant and the change in steepness are observed at the same frequency region. The phenomenon can be identified as interfacial polarization (IP) where the high values are presented at the low frequency region. At higher frequencies, the dipoles cause an inertia results from the electrical heterogeneity [21, 22], known as Maxwell-Wagner-Sillars effect [23]. With the rise in temperature, the dielectric loss is also increased. Two relaxation modes are observed in the 3D diagram of loss spectra of 4%ZnSe/PVA composites (fig. 6) in which at temperatures between 50^0C and 80^0C, an explicit relaxation peak is observed and identified as α – mode [24] that corresponds to micro-Brownian motion of the polymer chain. Next an expeditious peak is observed at around 110^0C and denoted as β – mode. It originates from the re-orientation of polar side group of the polymer chain that is attributed to the wriggling of hydroxyl groups. All the relaxation modes are also present in the plot of pure PVA.

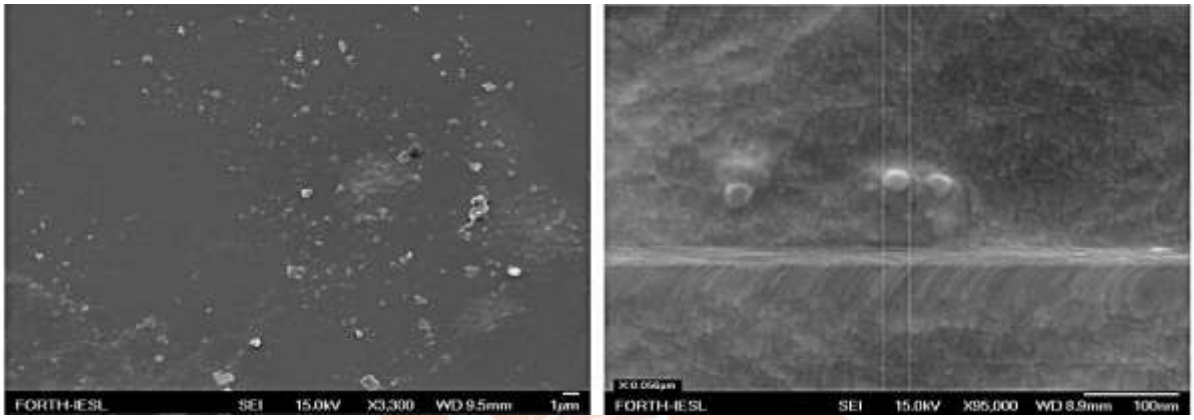

Fig. 2: SEM micrographs of 4%ZnSe/PVA nanocomposite at different magnification.

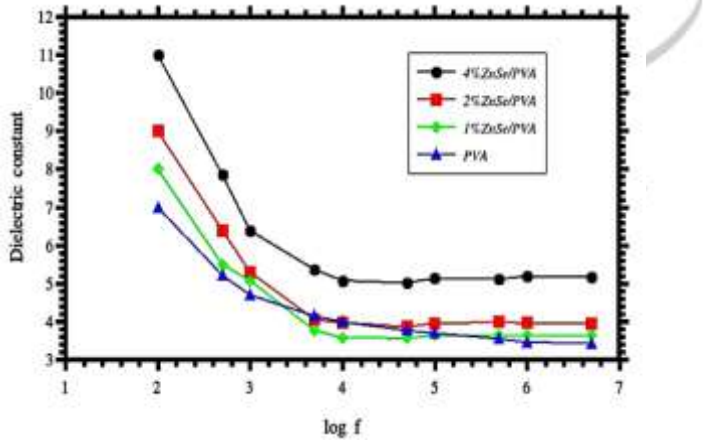

Fig. 3: The variation of dielectric constant vs. log f for pure PVA and composite samples.

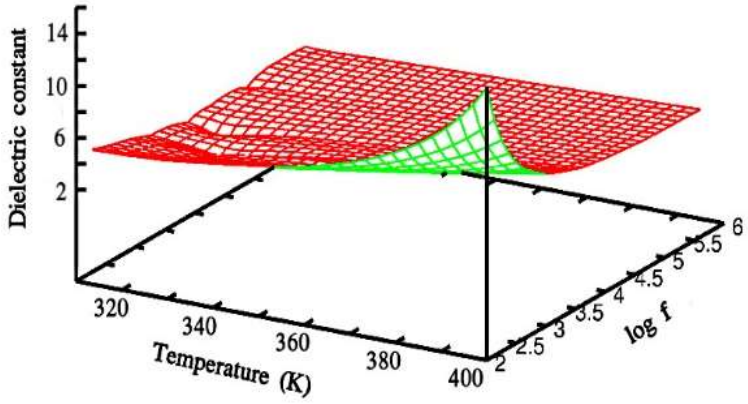

Fig. 4: The variation of dielectric constant of 4%ZnSe/PVA composite with temperature.

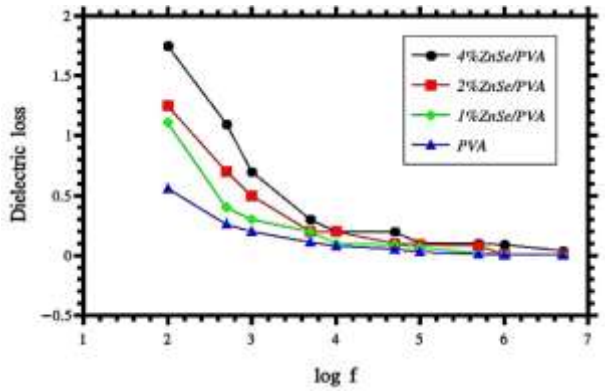

Fig. 5: The variation of dielectric loss vs. log f at room temperature.

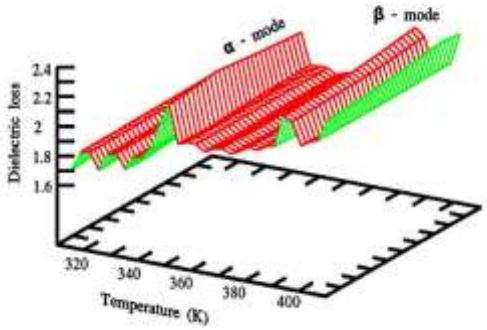

Fig. 6: The variation of dielectric loss of 4%ZnSe/PVA by varying temperature. 3D diagram pronounced the different relaxation peaks.

The complex electric modulus is defined by the reciprocal of the complex permittivity.

$$M^* = 1/\varepsilon^* = M' + j\,M''. \quad (1)$$

Where M^* is the complex modulus, ε^* is the complex permittivity, M' is the real part and M'' is the imaginary part of electric modulus. The complex modulus spectrum represents the measure of distribution of energies in the matrix and describes the electrical relaxation and microscopic properties of the material. The real and imaginary parts of electric modulus in accordance with frequency are described in fig. 7 and fig. 8 respectively. The value of the real part (M') is low at lower frequencies and moving to the higher frequencies, it increases and a saturated region is obtained. The value is higher for the pristine sample with comparison to the composite membranes but for the value of M'' which is increased in accordance with the filler inclusion. The frequency distribution is also different for imaginary electric modulus which shows a similar behavior as the dielectric loss spectra.

The curves of conductance (fig. 9) and impedance (fig. 10) are mutually connected. With the addition of ZnSe nanoparticles, the charge density is increased and these particles are relatively free to move in between the electrodes. So that a better conductance is noticed as the concentration of ZnSe is increased. It is confirmed from the impedance spectra that high impedance value is noticed for virgin PVA and it decreases with increasing concentrations of ZnSe particles. It can be also seen that the conductance increases but impedance decreases with the increase in frequency.

The energy storage of the dielectric materials is investigated to fulfill the dielectric measurements. The energy density is related to the dielectric permittivity and can be calculated as;

$$U = (\varepsilon_0\, \varepsilon_r\, E^2)/2. \quad (2)$$

Fig.11 presents a comparative diagram of the energy density of pure and ZnSe incorporated membranes at room temperature. The composite samples exhibit higher energy storage efficiency with comparison to the pure PVA. An increase of 5.3 % in the value of energy density is noticed in the case of 1% ZnSe doped PVA at 1 MHz and it reaches to 14.2 % and 49.7 % with 2% and 4% of ZnSe filler dispersion.

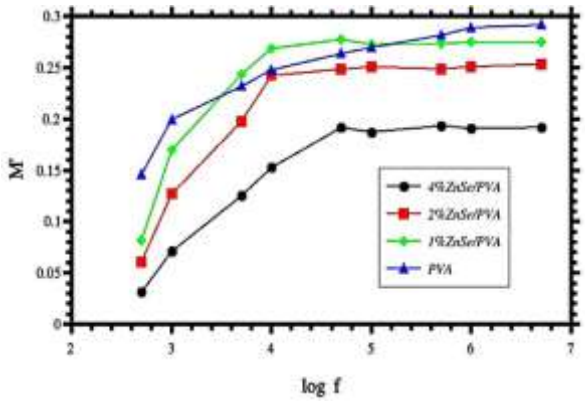

Fig. 7: The variation of real part of electric modulus in accordance with frequency.

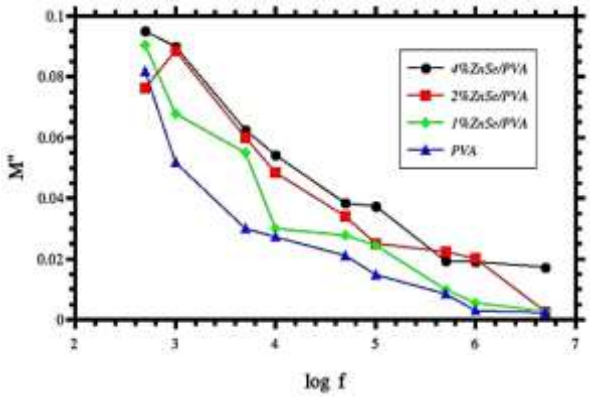

Fig. 8: The imaginary part of electric modulus vs. log f curve of PVA and its composites.

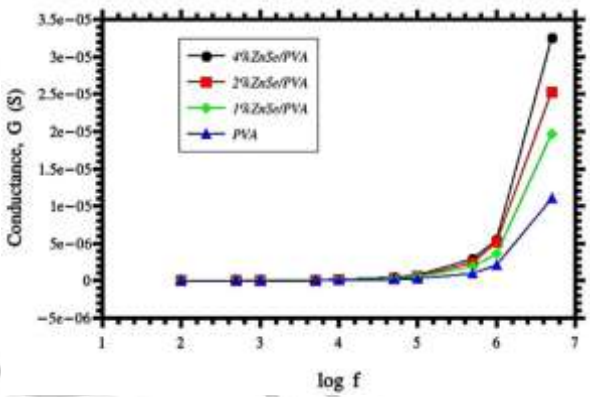

Fig. 9: The curve of conductance as a function of frequency of PVA and ZnSe/PVA.

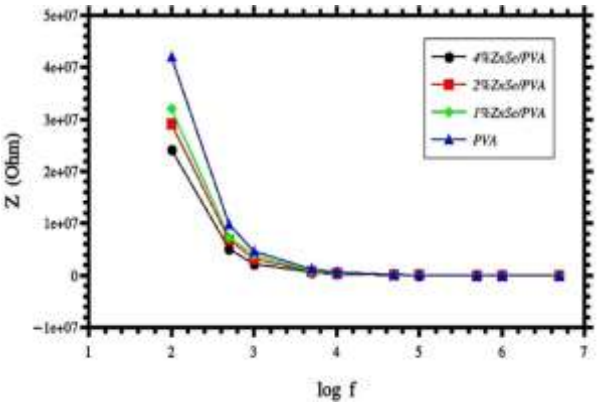

Fig. 10: The frequency dispersion of complex impedance of all samples.

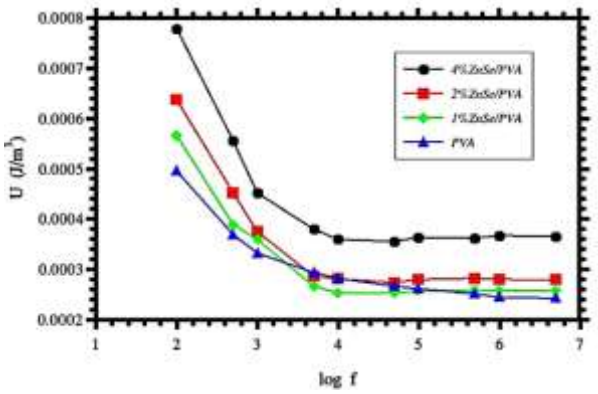

Fig. 11: A comparative diagram of the energy density of PVA and ZnSe/PVA membranes.

Optical properties

From UV- Vis- NIR absorption measurements, we can obtain the optical parameters such as absorption co-efficient (α), extinction co-efficient (*k*), index of refraction (*n*) and optical conductivity (σ_{opt}) by calculating reflectance *R* for all frequencies. Fig. 12 shows the absorbance spectra of PVA and ZnSe/PVA composite membranes. One can easily examine that all samples are transparent in the visible frequencies whereas a higher absorption has taken place in the UV region. It is perceived that the absorbance of the films increases with the increasing concentration of ZnSe particle which leads to an increase in light scattering losses. The observed decrease of absorbance with wavelength is due to the increase in crystalline size associated with higher densification of the films [25].

The absorption co-efficient (α) of the films strongly depends on optical transmission (*T*) and film thickness (*t*). The extinction co-efficient was obtained in terms of absorption co-efficient [26], $k = (\alpha \lambda)/ 4\pi$. Fig. 13 illustrates the behavior of the extinction co-efficient (*k*) vs. wavelength of PVA and its composites. The value is higher for composite films with the inclusion of ZnSe particles. This is due to the large values of absorption co-efficient of composites since α is directly proportional to the extinction coefficient. The average values are 0.0002, 0.0004, 0.0010 and 0.0015 respectively in the order of 0% to 4% of ZnSe incorporated PVA matrices. The plot of refractive index (*n*) and wavelength is shown in fig. 14. The estimated values of refractive index are almost constant in the entire wavelength for all samples. The values are increased in accordance with the filler inclusion. For pure PVA, it is 1.3 which increases up to 3.0 with 4% of ZnSe interaction. The obtained values are in good agreement with the values reported earlier for PVA based systems [27]. The high refractive index polymers (HRIP) are potential for the strong optical confinement and can enhance the optical intensities for non-linear interactions. The behavior of optical conductivity is also an independent wavelength trace except a tail is presented in the far UV region. It also increases with the filler inclusion and the high magnitude of optical conductivity confirms the photo response nature of the materials.

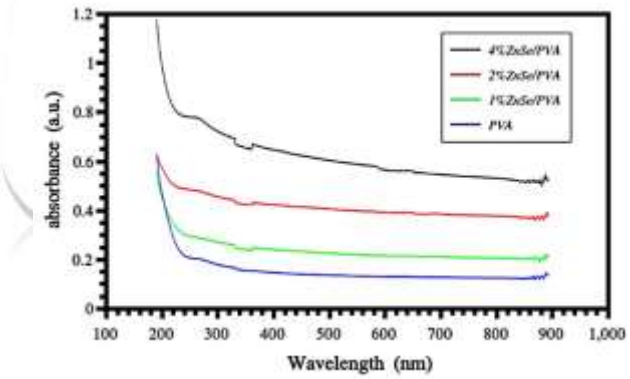

Fig. 12: UV- Vis- NIR absorption spectra of pure and doped samples.

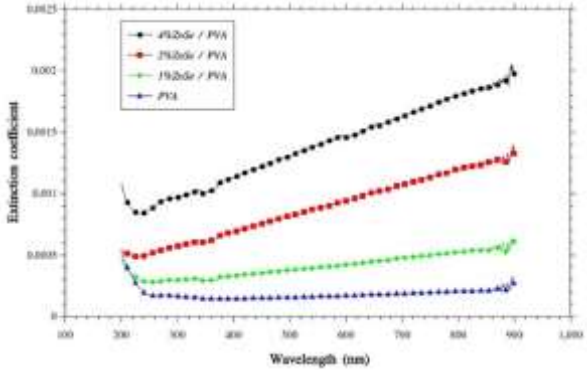

Fig. 13: The variation in the value of extinction co-efficient with different percentages of filler inclusion on PVA matrix.

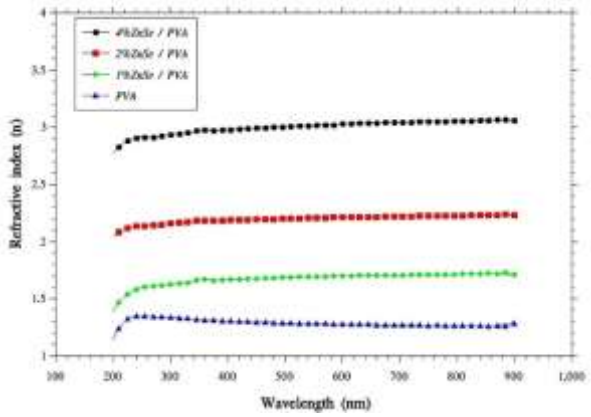

Fig. 14: The curve depicts the variation of refractive index corresponds to ZnSe inclusion.

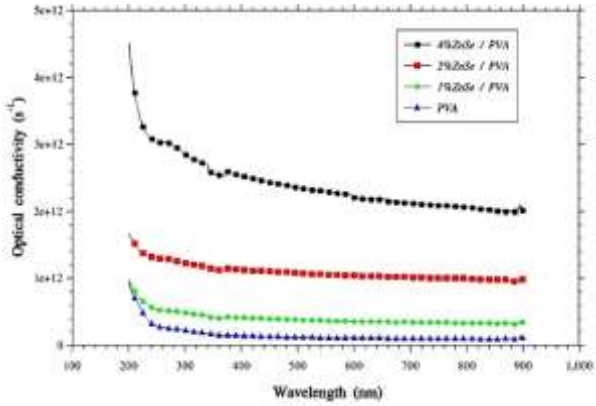

Fig. 15: The variation in the value of optical conductivity in the UV- Vis- NIR wavelength region.

The real part and imaginary part of complex permittivity are also calculated from the values of *n* and *k* in the wavelength 200 nm to 900 nm. It is inferred from fig. 16 that the values of relative permittivity are lesser for all the samples with comparison to the values in the radio frequency region which shows that there are some polarizations absent in the UV- Vis- NIR frequencies. In these regions, an independent frequency trace is noticed for all the samples and the value is increased for composites with the dopant concentration. The imaginary part of complex permittivity (shown in fig. 17) is also assented with the values obtained from the LCR analyzer. A frequency independent trace is noticed for pure PVA but it increases slightly with the wavelength for composite membranes.

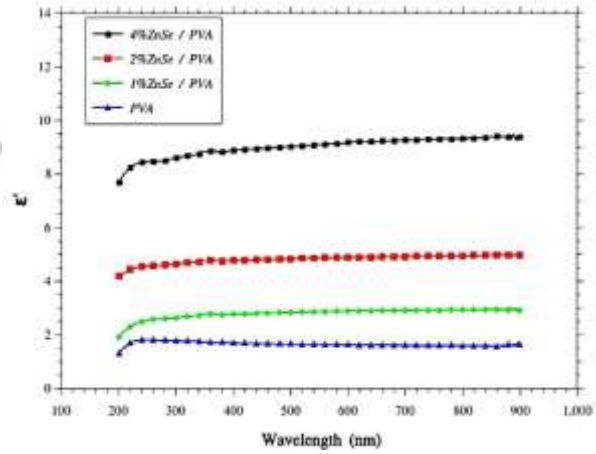

Fig. 16: The curve of real part of complex permittivity in UV- Vis- NIR frequency region.

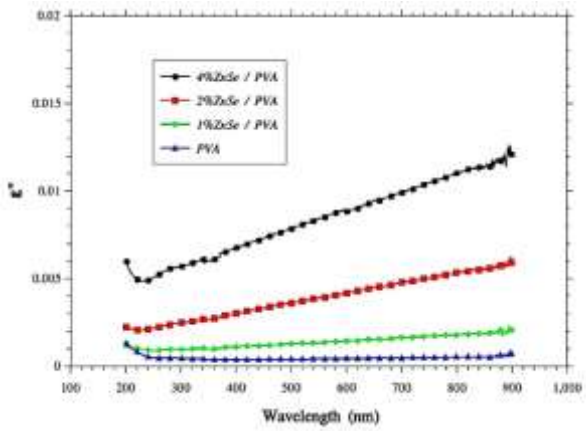

Fig. 17: The imaginary part of complex permittivity in UV- Vis- NIR frequency region for all samples.

IV. CONCLUSION

An authentic ultra-sonication technique for the preparation of ZnSe/PVA composite membranes could be established. The X-ray analysis revealed that the size of the prepared ZnSe was in nano-region and the dispersion of nanoparticles was analyzed with SEM micrographs. The dielectric measurement confirmed that the values of dielectric constant, dielectric loss and electric modulus were tailored with the inclusion of ZnSe nanoparticle. The real and imaginary parts of complex permittivity were also calculated in the UV- Vis- NIR frequencies and inferred that some polarizations are inactive. The dielectric relaxation phenomena were portrayed and the observed relaxation modes were α, β and IP which confirmed the electrical heterogeneity of the systems. The composite films exhibited a higher energy storage efficiency that is an increase of 49.7% (at 1MHz) was noticed in the case of 4% of ZnSe incorporated matrix. The extinction coefficient, index of refraction and optical conductivity could be enhanced with the dopant concentration.

REFERENCES

[1] J. Nunes-Pereiraa, V. Sencadas, V. Correia, J. G. Rochad, S. Lanceros-Mendez, "Energy harvesting performance of piezoelectric electrospun polymer fibers and polymer/ceramic composites," Sensor Actuat. A, vol. 196, pp. 55-62, 2013.
[2] S. Kea, Y. Yang, L. Ren, Y. Wang, Y. Li, H. Huang, "Dielectric behaviors of PHBHHx–$BaTiO_3$ multifunctional composite films," Compos. Sci. Technol, Vol. 72, pp. 370-375, 2012.
[3] C. V. Madhusudhana Rao, G. Prasad, "Characterization of piezoelectric polymer composites for MEMS devices," Bull. Mater. Sci, vol. 35, pp. 579-584, 2012.
[4]. X. J. Lin, K. C. Zhou, X. Y. Zhang, D. Zhang, "Development, modeling and application of piezoelectric fiber composites," Trans. Nonferr. Metall. Soc, vol. 23, pp. 98-107, 2013.
[5]. T. Lee, K. W. Kwok, H. L. Li, H. L. W. Chan, "Lead-free alkaline niobate-based transducer for ultrasonic wire bonding applications," Sensor Actuat. A, vol. 150, pp. 267-271, 2009.
[6] D. Zhou, K. H. Lam, Y. Chen, Q. Zhang, Y. C. Chiu, H. Luo, J. Dai, H. L. W. Chan, "Lead-free piezoelectric single crystal based 1–3 composites for ultrasonic transducer applications," Sensor Actuat. A, vol. 182, pp. 95-100, 2012.
[7] S. George, M. T. Sebastian, "Three-phase polymer–ceramic–metal composite for embedded capacitor applications," Compos. Sci. Technol, vol. 69, pp. 1298-1302, 2009.
[8]. Z. Zhang, H. Su, X. Tang, H. Zhang, T. Zhou, Y. Jing, "Glass-free low-temperature sintering and microwave dielectric properties of $CaWO_4 – Li_2WO_4$ ceramics," Ceram. Int, vol. 40, pp. 1613-1617, 2014.
[9]. S. Sathish, B. Chandar Shekar, B. T. Bhavyasree, "Nano composite PVA-TiO_2 thin films for OTFTs," Adv. Mater. Res, vol. 678, pp. 335-342, 2013.
[10] C. B. Murray, C. R. Kagan, M. G. Bawendi, "Self-organization of CdSe nanocrystallites into three-dimensional quantum dot super lattices," Science, vol. 270, pp. 1335-1338, 1995.
[11] A. P. Alivisatos, "Perspectives on the physical chemistry of semiconductor nanocrystals," J. Phys. Chem, vol. 100, pp. 13226-13239, 1996.
[12] P. V. Kamat, "Interfacial charge transfer processes in colloidal semiconductor systems," Prog. React. Kinet, vol. 19, pp. 277-316, 1994.
[13] A. P. Alivisatos, "Semiconductor clusters, nanocrystals and quantum dots," Science, vol. 271, pp. 933-937, 1996.
[14] H. Luo, J. K. Furdyna, "The II-VI semiconductor blue-green laser: challenges and solution," Semicond. Sci. Technol, vol. 10, pp. 1041-1048, 1995.
[15] P. Qi, Y. J. Dong, Y. D. Li, "ZnSe semiconductor hollow microspheres," Chem. Int. Ed, vol. 42, pp. 3027-3030, 2003.
[16] V. L. Colvin, M. C. Schlamp, A. P. Alivisatos, "Light-emitting-diodes made from cadmium selenide nanocrystals and a semiconducting polymer," Nature, vol. 370, pp. 354, 1994.
[17] W. C. W. Chan, S. Nie, "Quantum dot bio conjugates for ultrasensitive nonisotopic detection," Science, vol. 281, pp. 2016, 1998.
[18] I. V. Kityk, J. Kasperczyk, B. Sahraoui, M. F. Yasinskii, "Low temperature anomalies in polyvinyl alcohol photopolymers," Polymers 3, vol. 8, pp. 4803-4806, 1997.

[19] G. P. Mitchell, C. A. Mrkin, R. L. Letsinger, "Programmed assembly of DNA functionalized quantum dots," J. Am. Chem. Soc, vol. 121, pp. 8122-8123, 1999.
[20]. I. C. Baek, S. I. Seok, N. C. Pramanik, S. Jana, M. A. Lim, B. Y. Ahn, C. J. Lee, Y. J., "Ligand-dependent particle size control of PbSe quantum dots," J. Colloid Interface, vol. 310 (1), pp. 163-166, 2007.
[21]. N. Yahya, M. N. Akhtar, A. F. Mansuri, M. Kashif. "Synthesis and characterization of ZnO-CNT filled PVA composite as EM Detector," J. Appl. Sci, vol. 11(8), pp. 1303-1308, 2011.
[22]. H. Y. Chang, C. W. Lin., "Proton conducting membranes based on PEG/SiO_2 nanocomposites for direct methanol fuel cells," J. Membr. Sci, vol. 218, pp. 295-306, 2003.
[23]. H. Y. Chang, C. T. Lin, S. J. Chiu, "Preparation of the PVA/HAP composite polymer membrane for alkaline DMFC application," Desalination, vol. 233, pp. 137-146, 2008.
[24]. Soulintzis A. L., Kontos G. A., Karahaliou P. K., Psarras G. C., Georga S. N., Krontiras C. A., "Dielectric relaxation processes in epoxy resin-ZnO composites," J. Polym. Sci. Polym. Phys, vol. 47(4), pp. 445-54, 2009.
[25]. P. E. Agbo, M. N. Nnabuchi, "Core-shell TiO2/ZnO thin film: preparation, characterization and effect of temperature on some selected properties," Chalcogenide Lett, vol. 8, pp.273-282, 2011.
[26]. V. Kumar, T. P. Sharma, "Structural and optical properties of sintered ZnS_xSe_{1-x} films," Optical Materials, vol. 10, pp. 253-256, 1998.
[27]. S. Sugumaran, C. S. Bellan, "Transparent nano composite PVA-TiO_2 and PMMA-TiO_2 thin films: Optical and dielectric properties," Optik, vol. 125, pp. 5128-5133, 2014.